JOURNAL OF BACTERIOLOGY, Apr. 1998, p. 2021–2026 Vol. 180, No. 8
0021-9193/98/$04.00+0

Iron Uptake in *Ustilago maydis*: Tracking the Iron Path

ORLY ARDON,[1] RAPHAEL NUDELMAN,[2] CATHERINE CARIS,[2] JACQUELINE LIBMAN,[2]§ ABRAHAM SHANZER,[2] YONA CHEN,[3] AND YITZHAK HADAR[1]*

Department of Plant Pathology and Microbiology and The Otto Warburg Center for Agricultural Biotechnology[1] and Department of Soil and Water Sciences,[3] Faculty of Agricultural, Food and Environmental Quality Sciences, The Hebrew University of Jerusalem, and Department of Organic Chemistry, The Weizmann Institute of Science,[2] Rehovot 76100, Israel

Received 2 January 1998/Accepted 6 February 1998

In this study, we monitored and compared the uptake of iron in the fungus *Ustilago maydis* by using biomimetic siderophore analogs of ferrichrome, the fungal native siderophore, and ferrioxamine B (FOB), a xenosiderophore. Ferrichrome-iron was taken up at a higher rate than FOB-iron. Unlike ferrichrome-mediated uptake, FOB-mediated iron transport involved an extracellular reduction mechanism. By using fluorescently labeled siderophore analogs, we monitored the time course, as well as the localization, of iron uptake processes within the fungal cells. A fluorescently labeled ferrichrome analog, B9-lissamine rhodamine B, which does not exhibit fluorescence quenching upon iron binding, was used to monitor the entry of the compounds into the fungal cells. The fluorescence was found intracellularly 4 h after the application and later was found concentrated in two to three vesicles within each cell. The fluorescence of the fluorescently labeled FOB analog CAT18, which is quenched by iron, was visualized around the cell membrane after 4 h of incubation with the ferrated (nonfluorescent) compounds. This fluorescence intensity increased with time, demonstrating fungal iron uptake from the siderophores, which remained extracellular. We here introduce the use of fluorescent biomimetic siderophores as tools to directly track and discriminate between different pathways of iron uptake in cells.

Iron is an essential element for virtually all forms of life. Its solubility and bioavailability are extremely low under aerobic conditions at physiological pH. Microorganisms respond to iron limitation by secreting siderophores, low-molecular-weight compounds produced to solubilize, bind, and transport environmental iron to their cells (23).

Extracellular iron is transported across microbial cell membranes via different mechanisms (6, 27). The ferric siderophore transporter, or shuttle (31), involves a transporter or a permease for intact ferric siderophore complexes. After transport, iron is removed from the complex, and the desferrichelate is either secreted back into the medium (recycled) or destroyed by hydrolysis inside the cell. Another mechanism, usually referred to as the direct shuttle (6), or reductive and "taxicab" (5, 31), involves the uptake of iron after binding of the complex to a receptor on the cell surface without concomitant transport of the desferrisiderophore. In another proposed mechanism, iron is acquired extracellularly by an indirect shuttle, in which the reductive removal of the iron occurs at a site distant from the carrier protein (6).

Ustilago maydis, a maize pathogen, produces the siderophores ferrichrome and ferrichrome A (4), the same compounds first discovered in cultures of *Ustilago sphaerogena* (12, 21). It was demonstrated that cells of *U. maydis* can take up iron from ferrichrome as well as from biomimetic ferrichrome analogs (1). Biomimetic siderophore analogs were designed to mimic the essential features of the natural siderophores. The methodology for design involved modular assembly and was guided by theoretical calculations (26). Fluorescently labeled ferrichrome analogs were found to be useful tools in the study of microbial iron utilization (24, 28). The fluorescent analogs were prepared by conjugating the fluorescent probes at a site that does not interfere with the siderophore's iron binding domain or with the receptor recognition site. In general, the fluorescence of these analogs is quenched in the presence of ferric iron and is regained upon iron removal. Increased fluorescence in fungal cultures amended with the compounds is therefore a result of fungal utilization of the metal. The fluorescence increase of the anthracene-labeled ferrichrome analog B9-ANT in cultures of *U. maydis* was monitored and was found to correspond to ^{55}Fe-ferrichrome uptake (1). Fluorescence microscopy was used to further trace the fate of the deferrated siderophores. Fluorescence derived from the B9-ANT ligand was evident after 16 h of incubation in vesicles within *U. maydis* cells. Biological iron exchange processes were difficult to visualize and localize in vivo (19). The site and timing of iron removal from microbial siderophores have a major significance due to the crucial role of siderophores in microbial metabolism and pathogenicity.

In this report, we compare the uptake systems for ferrichrome-iron and for ferrioxamine B (FOB)-iron in *U. maydis* and demonstrate the use of fluorescent biomimetic analogs of these siderophores as tools to discriminate and track the pathway of iron uptake. Lissamine rhodamine B (LRB), which does not exhibit fluorescence quenching upon iron binding, was conjugated to the ferrichrome analog B9 (24). 4-Chloro-7-nitrobenzofurazane (NBD), a probe whose fluorescence is very sensitive to the presence of Fe^{3+}, was connected to the ferrioxamine derivative at the carboxylic end, thus retaining the essential free primary amine on the other end (25). The use of

* Corresponding author. Mailing address: Department of Plant Pathology and Microbiology and The Otto Warburg Center for Agricultural Biotechnology, The Hebrew University of Jerusalem, Faculty of Agricultural, Food and Environmental Quality Sciences, Rehovot 76100, Israel. Phone: 972 8 9481315. Fax: 972 8 9468785. E-mail: hadar@agri.huji.ac.il.

§ Jacqueline Libman passed away on March 30, 1997, while this work was in progress. This article is dedicated in her memory.

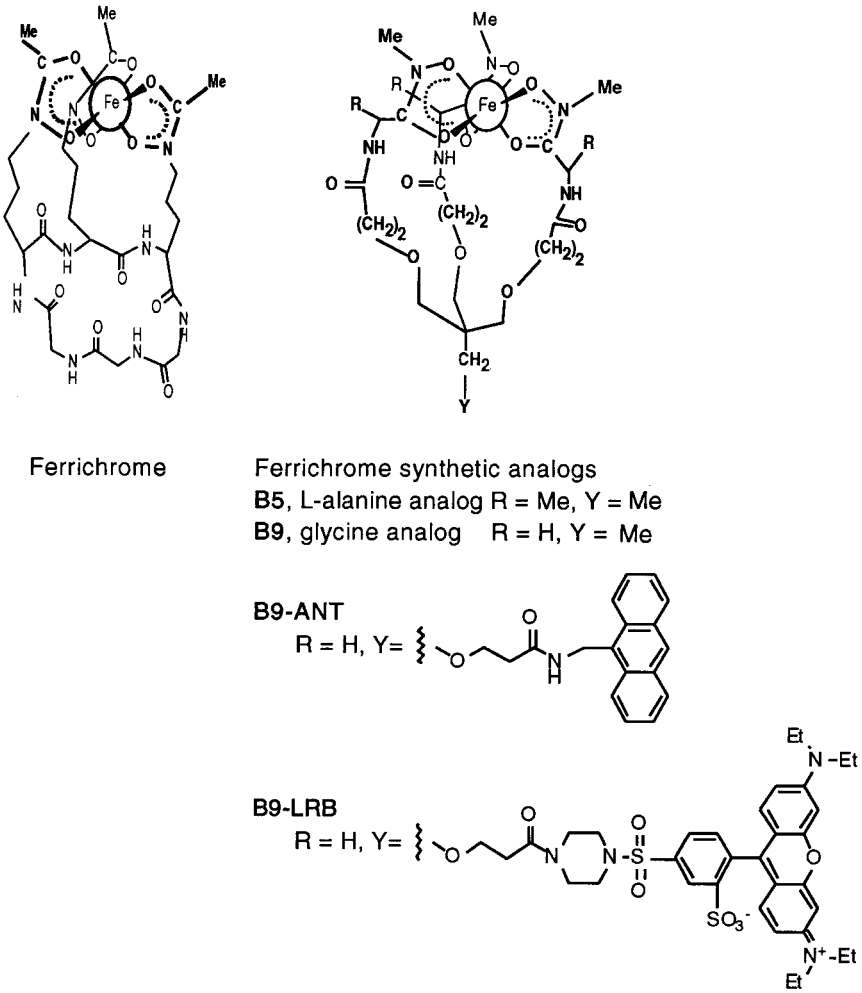

FIG. 1. Structures of ferrichrome and its synthetic analogs.

these analogs allowed us to monitor the time course and localization of iron uptake processes in the fungal cells.

MATERIALS AND METHODS

Fungal growth and maintenance. *U. maydis* Sid$^-$ mutant S023 (Sally Leong, Madison, Wis.) was grown in *Ustilago* medium as described previously (12), with a minor modification of a lower phosphate concentration (1 g/liter) for reducing the iron contamination in the medium. This mutant belongs to class II mutants, which are blocked in the biosynthesis of δ-*N*-hydroxyornithine (20). All glassware was washed in 5% HCl prior to autoclaving.

In growth curve studies, fungal cells were grown in 100-ml arm flasks, each containing 10 ml of *Ustilago* medium. The Fe^{3+} chelates were added to a final concentration of 1 μM. The flasks were inoculated with the fungal cells and shaken at 28°C and 150 rpm. Growth was measured by following turbidity at 620 nm. Each treatment was conducted in duplicate, and the experiment was repeated three times.

Siderophores. Ferrichrome was purchased from Sigma (St. Louis, Mo.). Structures of the biomimetic ferrichrome analogs and their fluorescent derivatives are shown in Fig. 1. L-Alanine-based ferrichrome analog B5 and glycine-based analog B9 were synthesized as described previously (2). Fluorescently labeled analog B9-LRB was synthesized as described by Nudelman et al. (24). FOB was purchased from Ciba-Geigy (Switzerland) as Desferal. Structures of fluorescently labeled FOB analogs used in this study are shown in Fig. 2. NBD-FOB (16) and CAT18 (25) were synthesized as described previously. The siderophores were complexed with Fe^{3+} by using $FeCl_3$ to 90% saturation, equilibrated for 24 h, and then filtered through a 0.2-μm-pore-size filter. All stock solutions were kept frozen in the dark.

^{55}Fe uptake studies. Cultures grown for 2 to 3 days at 28°C and 150 rpm were centrifuged for 15 min at 3,000 × *g*, resuspended in fresh half-strength standard succinate medium, to a final absorbance of 1.5 at 620 nm, and preincubated for 60 min at 30°C. ^{55}Fe was purchased as $^{55}FeCl_3$ from Amersham International, Amersham, United Kingdom. The labeled ^{55}Fe-siderophore complex was added to a final concentration of 1 μM. At specified time points, aliquots (0.5 ml) were taken in duplicate, layered onto a mixture of dibutyl phthalate-dioctyl phthalate (1/1, vol/vol; Sigma), and centrifuged. The supernatant was removed, and the Eppendorf tube tips were cut. Radioactivity in the tips of the tubes containing the fungal cells was counted on a Beckman LS1801 counter, using Insta Gel II as the scintillation mixture. Results presented are averages of three experiments.

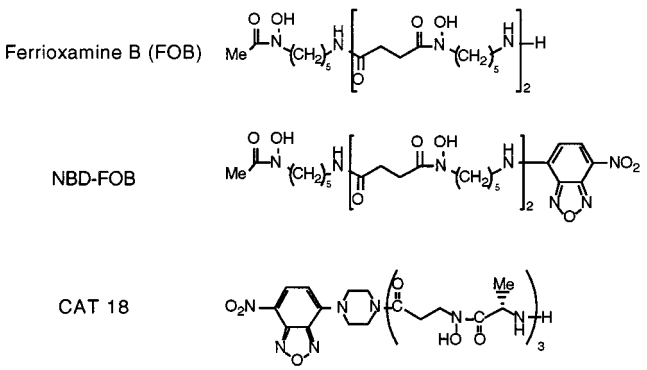

FIG. 2. Structures of FOB and its fluorescently labeled synthetic analogs.

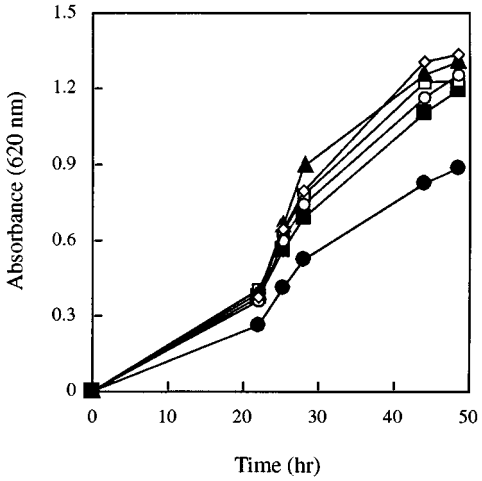

FIG. 3. *U. maydis* S023 growth curve in media amended with five iron complexes (1 μM): $FeCl_3$ (◇), ferrichrome (○), FOB (▲), B5 (□), and B9 (■). ●, control. The data shown are mean values of three separate experiments (standard deviation up to 12%).

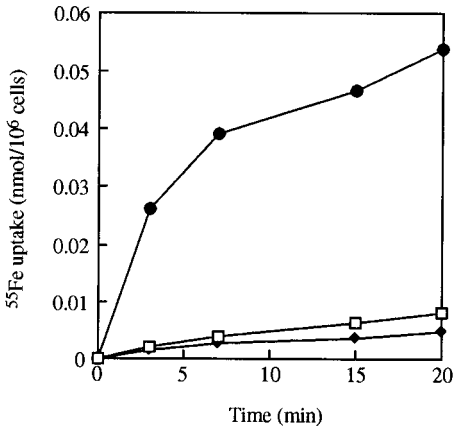

FIG. 4. Siderophore-iron uptake in *U. maydis* S023 from 1 μM ^{55}Fe-FOB (□), ^{55}Fe-CAT18 (◆), and ^{55}Fe-ferrichrome (●). The data shown are mean values of three separate experiments (standard deviation up to 16%).

Fluorometry. For fluorescence studies, the cells were grown and prepared as described above. The ferrated fluorescently labeled siderophore analog was added to the fungal suspension to a final concentration of 5 μM. Aliquots of 1 ml were drawn at specified time points and centrifuged, and the supernatant was collected. Fluorescence emission was measured at 548 nm by excitation at 475 nm, using an SLM Instruments fluorometer (model 4800). Results are presented in arbitrary units of fluorescence. Each experiment was conducted in duplicate and repeated three times.

Extracellular iron reductase assay. Reduction of Fe^{3+} was monitored by using the Fe^{2+} chelator BPDS (baptophenanthroline disulfonate) (14). *U. maydis* was grown for 2 days and centrifuged, and the cells were dispersed in 50 mM Tris buffer (pH 7.5) to an absorbance of 1 at 620 nm. A 1-ml reaction mixture contained 900 μl of the cell suspension, 10 mM BPDS, and the ferrated siderophores at different concentrations. The formation of the Fe^{2+}-BPDS complex was monitored spectrophotometrically at 540 nm for 15 min. Background levels were determined by using parallel samples with cell extract. These readings were subtracted from the values obtained with samples containing fungal cells. Results are given as iron reduction rates.

Fluorescence confocal microscopy. The siderophore was added to a 2-ml fungal suspension to a final concentration of 50 μM, and samples were taken at different time intervals. Cells were observed by using a Leica TCS4D system (Leitz, Heidelberg, Germany) with a 100× 1.3 oil immersion objective. Fluorescence filter combinations used were as follows: for NBD-FOB and CAT18, λ_{ex} = 488 nm, dichroic/double dichroic 488/568 nm as a beam splitter, and LP filter 515 as a barrier filter; for B9-LRB, λ_{ex} = 568 nm, double dichroic 488/568 nm as a beam splitter, and LP filter 515 as a barrier filter.

RESULTS

Growth in iron-supplemented medium. To study the effectiveness of different sources of iron in promoting *U. maydis* growth, the fungus was grown on low-iron media containing different iron sources. Growth rates of all cultures treated with iron were higher than those of the control (Fig. 3). Fungal growth in media amended with ferrichrome was not significantly different from its growth rate in media supplemented with the ferrichrome analogs B5 and B9, FOB, or $FeCl_3$. The amendment of Fe-EDTA or Fe-ethylenediamine-di(*o*-hydroxyphenylacetic acid (EDDHA) to fungal cultures resulted in growth curves similar to those for the other iron sources (data not shown). The growth curves obtained with natural and/or synthetic iron sources demonstrated the ability of this fungus to extract iron from various ferric complexes. Since the fungal strain used was a Sid^- mutant, growth ability of the cells in iron-poor media amended with different iron sources suggests direct utilization of the iron supplied and rules out the possibility of ligand exchange with the native siderophores.

Iron uptake from FOB. Ferrioxamines are siderophores produced by most actinomycetal strains but not by *U. maydis* or other fungi (22). To confirm FOB-mediated iron uptake by the fungal cells, experiments testing ^{55}Fe uptake from FOB and its fluorescent analog CAT18 were conducted. The uptake rates were compared to ferrichrome-mediated ^{55}Fe uptake rates. Incubation of *U. maydis* with 1 μM ^{55}Fe-labeled siderophore complexes (Fig. 4) resulted in iron uptake from FOB and CAT18 as well as from ferrichrome. After 20 min of incubation, uptake of ^{55}Fe from FOB and CAT18 reached levels of 0.0082 and 0.0058 nmol/10^6 cells, respectively, whereas ferrichrome mediated ^{55}Fe uptake at a significantly higher rate, totaling 0.0538 nmol/10^6 cells. This result suggests higher Fe uptake efficiency of the fungus when the Fe is mediated by its native siderophore rather than an exogenous one.

Extracellular Fe-reductase activity. To further characterize the mechanism of Fe uptake from FOB by the fungus, extracellular Fe-reductase activity was monitored. Ferric reductase activity was measured by the extracellular accumulation of the BPDS ferrous complex. The $Fe^{3+} \rightarrow Fe^{2+}$ reduction rates measured for FOB and ferrichrome ferric complexes at a concentration of 100 μM were 0.314 and 0.001 μmol/h/10^6 cells, respectively. The difference in rates prevailed over a concentration range of 1 to 180 μM. From these observations, we concluded that an extracellular reductive dissociation is involved in iron uptake from FOB-type compounds, while a different mechanism which does not require extracellular reduction, for example, the shuttle mechanism, is responsible for uptake of iron from ferrichrome-type compounds.

Iron utilization from fluorescently labeled FOB analogs. The NBD-labeled ferrioxamine analog CAT18 was used as a dynamic probe to monitor FOB-mediated Fe uptake by the fungal cells and determine its localization. In the fluorescence studies, fungal cells were incubated with the ferrated siderophores, which are nonfluorescent in their Fe complex state and fluorescent in the free ligand form. Therefore, once iron is removed from the complex, an increase in fluorescence can be measured in the medium. The ligands used were found to be stable under the experimental conditions used. This approach was found to provide novel information on Fe uptake and localization as was previously shown with the fluorescent ferrichrome siderophore analog B9-ANT (1). Incubation of *U. maydis* S023 cells with CAT18 at a concentration of 5 μM resulted in an increase in fluorescence in the culture filtrate

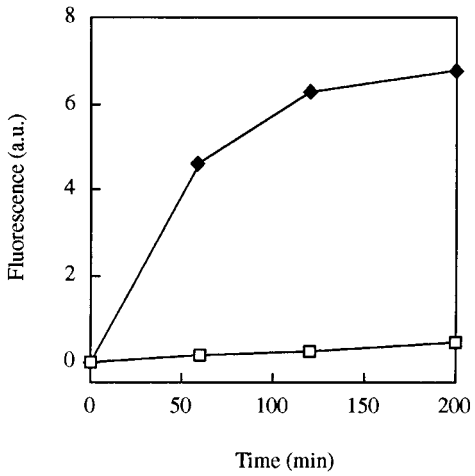

FIG. 5. Fluorescence increase in cultures of *U. maydis* S023 amended with Fe-CAT18, a fluorescent analog of FOB, at a concentration of 5 μM (◆) and in control samples (□). The data shown are mean values of three separate experiments (standard deviation up to 15%).

(Fig. 5), demonstrating utilization of the chelated iron. A concentration-dependent iron utilization experiment with CAT18 revealed saturation kinetics with maximal activity at a siderophore concentration of 5 μM.

Fluorescence studies of the iron exchange pathway. In vivo localization of the biomimetic siderophores B9-LRB and CAT18 was determined in cells of *U. maydis* by fluorescence microscopy.

We studied the site of fungal iron uptake from the FOB analog by incubating the fungal cells with Fe-quenchable CAT18. An increase of fluorescence, corresponding to an increase in the nonferrated siderophore concentration, was observed as early as 4 h after the beginning of incubation with the CAT18 ferric complex (Fig. 6e). The fluorescence can be seen around the cell, presumably between the membrane and the cell wall. After 18 h (Fig. 6f), the fluorescence intensified around the membrane, and the same pattern was observed after 48 h (Fig. 7b). Fluorescence could not be traced within the cells at all times, indicating no intracellular uptake of the ligand by *U. maydis*. Similar qualitative results were found for NBD-FOB, although its fluorescent signal was weaker than that obtained with CAT18.

In an earlier study (1), we monitored the fluorescence derived from the anthracene-labeled ferrichrome analog B9-ANT in cells of *U. maydis*. The fluorescent label was observed after 16 h of incubation in regularly shaped vesicles within the fungal cell. In the present study, LRB-labeled B9, a compound in which the fluorescence is not quenched by iron, was used (24). This unique property allowed us to follow the pathway of the siderophore uptake from the initial stages, when iron is still complexed, to consequential localized concentration within the

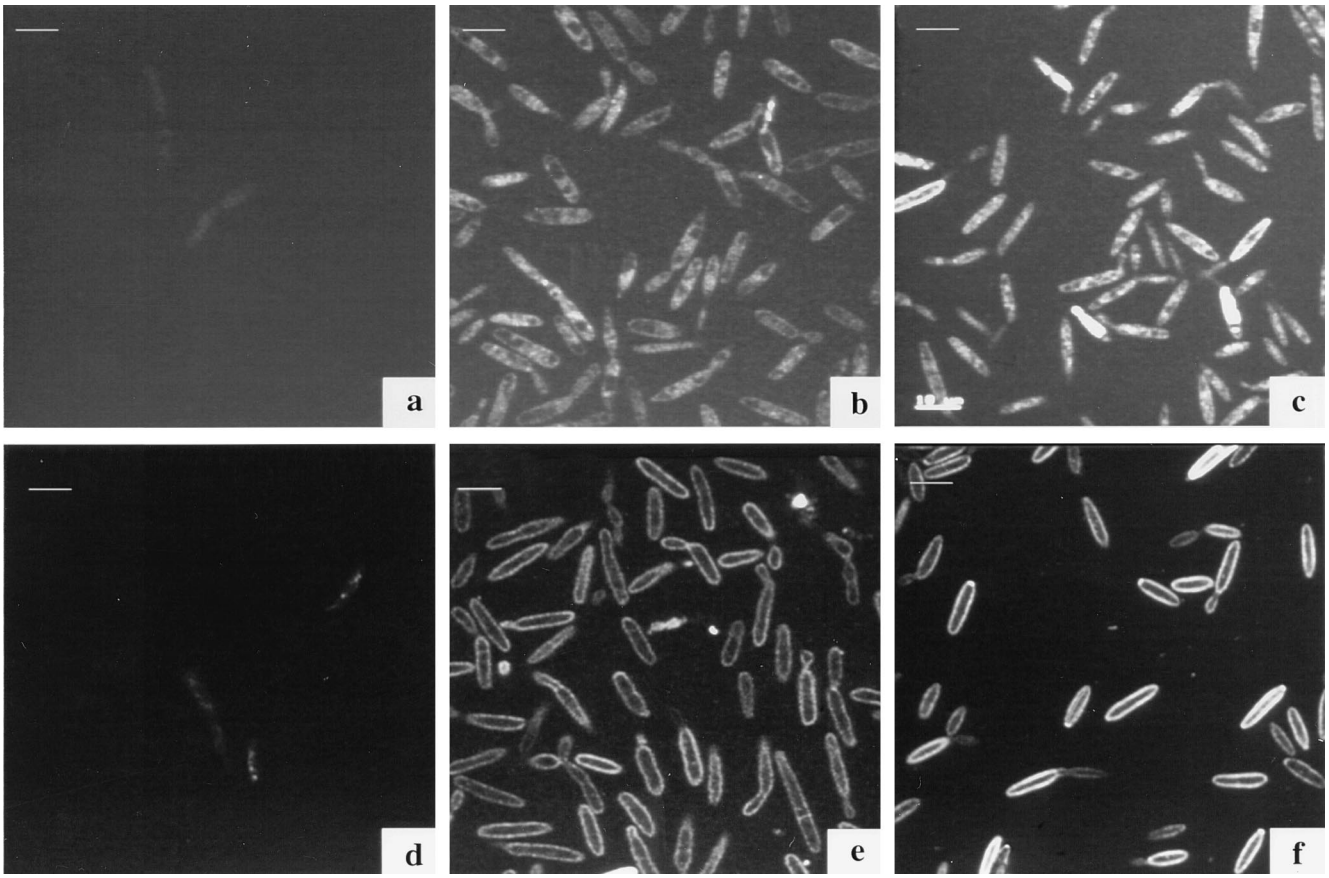

FIG. 6. Confocal micrographs of *U. maydis* S023 incubated with 50 μM Fe-B9-LRB (a to c) and Fe-CAT18 (d to f). Fluorescence label can be seen within cells treated with the fluorescent ferrichrome analog (B9-LRB) in comparison with an increase of fluorescence around the cell membranes with the FOB analog CAT18. (a and d) Control; (b and e) after 4 h of incubation; (c and f) after 18 h of incubation. Images were acquired with a Leica TCS4D system and processed by using Adobe Photoshop software on a Power Macintosh computer. Bars, 10 μm.

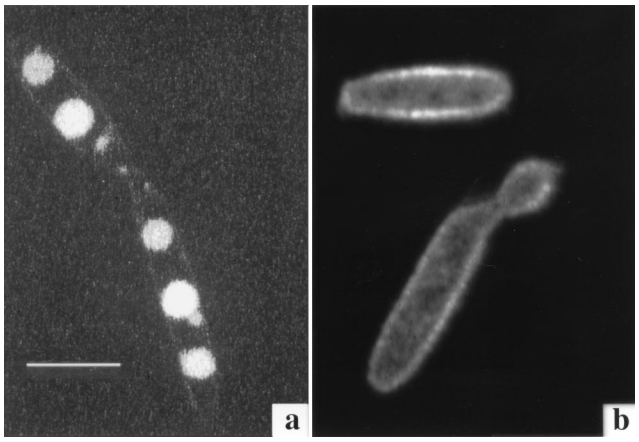

FIG. 7. Confocal micrographs of *U. maydis* S023 incubated for 48 h with 50 μM Fe-B9-LRB (a) and Fe-CAT18 (b). Fluorescence derived from the ferrichrome analog (B9-LRB) is clearly concentrated in vesicles within the cell, whereas fluorescence derived from the FOB analog CAT18 is localized around the cell membrane. Images were acquired as for Fig. 6. Bar, 10 μm.

fungal cell. A time course experiment monitoring iron utilization by the fungal cells via confocal microscopy was conducted. Cells of *U. maydis* were incubated with B9-LRB, washed, and mounted on microscopic slides. Photographs were captured at 0, 4, 18 (Fig. 6a to c), and 48 (Fig. 7a) h following the onset of incubation. The fluorescent label of B9-LRB was first seen around the membrane at 4 h of incubation (Fig. 6b); after longer incubation periods (Fig. 6c), more fluorescence was observed inside the cell, in regularly shaped organelles. A comparison of these observations to those of our previous studies using B9-ANT (1) suggests that at least some of the B9-LRB molecules found in the vesicles at this stage (18 h) are in a nonferrated state. After 48 h (Fig. 7a), the fluorescence is clearly localized in two to three vesicles within each cell.

DISCUSSION

U. maydis, a ferrichrome producer, is capable of taking up iron from various mineral and organic iron sources. FOB, originally isolated from *Streptomycetes pilosus* and bacteria (22), was also found to promote growth of this fungus in iron-limited media. ^{55}Fe uptake from FOB was only 15% of that of ferrichrome (Fig. 4), suggesting that in *U. maydis*, recognition and/or the transport system of the native siderophore is more efficient than that of the nonnative compound. In *U. sphaerogena*, ferrichrome was found to act as a recyclable shuttle in transporting iron into and within the fungal cells, while the second siderophore produced by this fungus, ferrichrome A, was found to function extracellularly as a taxi molecule, bringing iron to the cell surface but not normally crossing the membrane (9).

In an earlier study (1), we applied ferrichrome analogs for iron uptake studies in *U. maydis*. The use of the ferrichrome analog B9-ANT, which turns fluorescent upon iron removal, facilitated a direct study of iron utilization pathways by the fungal cells both fluorometrically and microscopically. The fluorescence derived from the deferrated fluorescent siderophores was found in vesicles within the fungal cells, confirming the shuttle mechanism for ferrichrome analogs in this fungus.

The existence of another, nonspecific reductive mechanism of obtaining iron from its chelated forms in *Ustilago* has been suggested by Emery (11). In this system, chelated iron is reduced to its divalent state prior to the transfer of the metal across the membrane. This additional strategy allows microorganisms to utilize iron from nonspecific sources such as siderophores produced by other microorganisms and provides them with an ecological advantage by competing for iron in various environments.

In this study, FOB-mediated iron uptake was found to involve an extracellular ferric reduction mechanism. In plants (3) and *Saccharomyces cerevisiae* (14), the extracellular reduction system has a low substrate specificity. Lodge (15) suggested that this feature enables a microorganism to reduce Fe^{3+} not only from its natural chelate but also from exogenous iron sources.

In the yeast *S. cerevisiae*, which does not produce siderophores, the mechanism for FOB-mediated iron uptake was found to involve internalization of the complex via a specific high-affinity transport system (14). A variety of other iron sources including ferrichrome were examined, but an additional specific transport system was not found (13). Two transport systems which depend on the activity of surface ferrireductases coexist with the siderophore-mediated transport system and serve as the main iron uptake mechanism at least under laboratory conditions. These systems have been studied and characterized (7, 8, 10).

Traditional iron uptake studies use techniques such as isotope-labeled siderophores and atomic absorption, with electron spin resonance and Mössbauer spectroscopic measurements as complementary methods (30). Since all of the methods that have been described enable one to follow the uptake of either iron or its chelate, an analysis of the kinetics of double-labeled siderophore uptake is used for investigating the mechanism of siderophore-mediated iron transport (30). Fluorescently labeled biomimetic siderophores were found to be suitable tools for iron uptake studies in microorganisms (1, 24, 28).

Fluorescently labeled FOB analogs were designed, synthesized, and tested for activity in vivo in this research. As in B9-ANT (1), their fluorescence is quenched upon complexation with ferric ions, thus allowing the distinction between the Fe-loaded siderophore and the free ligand. This property allowed us to perform a real-time microscopic study and determine the localization of iron removal from Fe-CAT18. This FOB-biomimetic compound remained extracellular, as was evident by the increase of fluorescence intensity around the cell membrane throughout the 48-h incubation of the compound with the fungal cells. By using the nonquenchable ferrichrome analog B9-LRB, we were able to follow the pathway of the iron-loaded siderophore into the cell. In contrast to the FOB analog, the ferrichrome analog was visualized intracellularly and was eventually found concentrated in regularly shaped organelles. In our earlier studies with B9-ANT (1), we visualized the fluorescence label (i.e., iron removal) only 16 h after the beginning of the incubation with the fungal culture. Taken together, these results suggest that after 18 h, at least part of the molecules of B9-LRB which were observed in the vesicles are in a deferrated state. The lag between the labeled-iron uptake and fluorescence appearance in vesicles when B9-ANT was used was suggested to stem from a short-term iron storage role for ferrichrome in this fungus. A storage role was proposed earlier for natural siderophores in different microbial systems (17, 18, 29). Sequential intracellular iron reduction and export of the ligand for recycling outside the cell would be expected to follow ferrichrome uptake as a function of the metabolic requirements for the metal.

In this study, we followed and compared the uptake of iron in *U. maydis* from ferrichrome, the fungal native siderophore, and from FOB, a xenosiderophore, and their analogs. The time

course and in vivo localization of iron uptake processes were monitored. We further demonstrated the usefulness of a variety of fluorescent probes conjugated to biomimetic siderophores as tools for direct discrimination and in vivo tracking of different pathways of iron uptake in cells.

ACKNOWLEDGMENTS

We thank Sally Leong, USDA/ARS and University of Wisconsin, for providing fungal strains; Werner Knebel and Wild-Leitz Instruments, Heidelberg, Germany, for providing the confocal microscope facilities; and Gabrielle Schneider for technical assistance in operating the microscope. We thank Tzili Sadowski for help in processing of the pictures.

This work was partly supported by the U.S.-Israel Binational Agricultural Research and Development Fund.

REFERENCES

1. **Ardon, O., H. Weizman, J. Libman, A. Shanzer, Y. Chen, and Y. Hadar.** 1997. Iron uptake in *Ustilago maydis*: studies with fluorescent ferrichrome analogues. Microbiology **143:**3625–3631.
2. **Berner, I., P. Yakirevitch, J. Libman, A. Shanzer, and G. Winkelmann.** 1991. Chiral linear hydroxamates as biomimetic analogues of ferrioxamine and their use in probing siderophore-receptor specificity in bacteria and fungi. Biol. Metals **4:**186–191.
3. **Bienfait, H. F.** 1989. Prevention of stress in iron metabolism of plants. Acta Bot. Neerl. **38:**105–129.
4. **Budde, A. D., and S. A. Leong.** 1989. Characterization of siderophores from *Ustilago maydis*. Mycopathologia **108:**125–133.
5. **Carrano, C. J., and K. N. Raymond.** 1978. Coordination chemistry of microbial iron transport compounds: rhodotorulic acid and iron uptake in *Rhodotorula pilmanae*. J. Bacteriol. **136:**69–74.
6. **Crowley, D. E., Y. C. Wang, C. P. P. Reid, and P. J. Szaniszlo.** 1991. Mechanisms of iron acquisition from siderophores by microorganisms and plants. Plant Soil **130:**179–198.
7. **Dancis, A., D. G. Roman, G. J. Anderson, and A. G. Hinnebusch.** 1992. Ferric reductase of *Saccharomyces cerevisiae*: Molecular characterization, role in iron uptake, and transcriptional control by iron. Proc. Natl. Acad. Sci. USA **89:**3869–3873.
8. **De Silva, D. M., C. C. Askwith, and J. Kaplan.** 1996. Molecular mechanisms of iron uptake in eukaryotes. Physiol. Rev. **76:**31–47.
9. **Ecker, D. J., C. W. Passavant, and T. Emery.** 1982. Role of two siderophores in *Ustilago sphaerogena*. Biochim. Biophys. Acta **720:**242–249.
10. **Eide, D., S. Davis-Kaplan, I. Jordan, D. Sipe, and J. Kaplan.** 1992. Regulation of iron uptake in *Saccharomyces cerevisiae*. J. Biol. Chem. **267:**20774–20781.
11. **Emery, T.** 1987. Reductive mechanisms of iron assimilation, p. 235–250. *In* G. Winkelmann, D. van der Helm, and J. B. Neilands (ed.), Iron transport in microbes, plants and animals. VCH Chemie, Weinheim, Germany.
12. **Garibaldi, J. A., and J. B. Neilands.** 1955. Isolation and properties of ferrichrome A. J. Am. Chem. Soc. **77:**2429–2430.
13. **Lesuisse, E., and P. Labbe.** 1994. Reductive iron assimilation in *Saccharomyces cerevisiae*, p. 149–179. *In* G. Winkelmann and D. R. Winge (ed.), Metal ions in fungi. Marcel Dekker, Inc., New York, N.Y.
14. **Lesuisse, E., F. Raguzzi, and R. R. Crichton.** 1987. Iron uptake by the yeast *Saccharomyces cerevisiae*: involvement of a reduction step. J. Gen. Microbiol. **133:**3229–3236.
15. **Lodge, J. S.** 1993. Enzymatic reduction of iron in siderophores, p. 241–250. *In* L. L. Barton and B. C. Hemming (ed.), Iron chelation in plants and soil microorganisms. Academic Press, San Diego, Calif.
16. **Lytton, S. D., Z. I. Cabantchik, J. Libman, and A. Shanzer.** 1991. Reversed siderophores as antimalarial agents. II. Selective scavenging of Fe(III) from parasitized erythrocytes by a fluorescent derivative of Desferal. Mol. Pharmacol. **40:**584–590.
17. **Matzanke, B. F., E. Bill, A. X. Trautwein, and G. Winkelmann.** 1987. Role of siderophores in iron storage in spores of *Neurospora crassa* and *Aspergillus ochraceus*. J. Bacteriol. **169:**5873–5876.
18. **Matzanke, B. F., E. Bill, A. X. Trautwein, and G. Winkelmann.** 1990. Siderophores as iron storage compounds in the yeasts *Rhodotorula minuta* and *Ustilago sphaerogena* detected by in vivo Mössbauer spectroscopy. Hyperfine Interact. **58:**2359–2364.
19. **Matzanke, B. F., G. Müller-Matzanke, and K. N. Raymond.** 1989. Siderophore-mediated iron transport, p. 3–121. *In* H. B. Gray and B. P. Lever (ed.), Iron carriers and iron proteins. VCH, Weinheim, Germany.
20. **Mei, B., A. D. Budde, and S. A. Leong.** 1993. *sid1*, a gene initiating siderophore biosynthesis in *Ustilago maydis*: molecular characterization, regulation by iron, and role in phytopathogenicity. Proc. Natl. Acad. Sci. USA **90:**903–907.
21. **Neilands, J. B.** 1952. A crystalline organo-iron pigment from a rust fungus (*Ustilago sphaerogena*). J. Am. Chem. Soc. **74:**4846–4847.
22. **Neilands, J. B.** 1981. Microbial iron compounds. Annu. Rev. Biochem. **50:**715–731.
23. **Neilands, J. B., K. Konopka, B. Schwyn, M. Coy, R. T. Francis, B. H. Paw, and A. Bagg.** 1987. Comparative biochemistry of microbial iron assimilation, p. 3–34. *In* G. Winkelmann, D. van der Helm, and J. B. Neilands (ed.), Iron transport in microbes, plants and animals. VCH Chemie, Weinheim, Germany.
24. **Nudelman, R., O. Ardon, Y. Hadar, Y. Chen, J. Libman, and A. Shanzer.** Modular fluorescent-labeled siderophore analogs. J. Med. Chem., in press.
25. **Nudelman, R., C. Caris, H. Weizman, O. Ardon, J. Libman, Y. Hadar, Y. Chen, and A. Shanzer.** 1996. Fluorescent-labeled siderophore analogs. Biosensors for the imaging of iron-exchange processes. Presented at European Research Conferences, August 29 to September 3, Salamanca, Spain.
26. **Shanzer, A., and J. Libman.** 1996. From biomimetic ion carriers to helical structures. Croat. Chem. Acta **69:**709–729.
27. **van der Helm, D., and G. Winkelmann.** 1994. Hydroxamates and polycarboxylates as iron transport agents (siderophores) in fungi, p. 39–98. *In* G. Winkelmann and D. R. Winge (ed.), Metal ions in fungi. Marcel Dekker, Inc., New York, N.Y.
28. **Weizman, H., O. Ardon, B. Mester, J. Libman, O. Dwir, Y. Hadar, Y. Chen, and A. Shanzer.** 1996. Fluorescently-labeled ferrichrome analogs as probes for receptor-mediated, microbial iron uptake. J. Am. Chem. Soc. **118:**12368–12375.
29. **Winkelmann, G.** 1991. Recent advances in uptake and storage of iron in fungi, p. 233–238. *In* Y. Chen and Y. Hadar (ed.), Iron nutrition and interactions in plants. Kluwer Academic Publishers, Dordrecht, The Netherlands.
30. **Winkelmann, G.** 1991. Specificity of iron transport in bacteria and fungi, p. 65–106. *In* G. Winkelmann (ed.), Handbook of microbial iron chelates. CRC Press, Boca Raton, Fla.
31. **Winkelmann, G.** 1993. Kinetics, energetics, and mechanisms of siderophore iron transport in fungi, p. 219–239. *In* L. L. Barton and B. C. Hemming (ed.), Iron chelation in plants and soil microorganisms. Academic Press Inc., San Diego, Calif.